

Surface friction alters the agility of a small Australian marsupial

Rebecca Wheatley^{*a}, Christofer J. Clemente^b, Amanda C. Niehaus^a,

Diana O. Fisher^a & Robbie S. Wilson^a

^a School of Biological Sciences, University of Queensland, Brisbane, Australia

^b School of Science and Engineering, University of the Sunshine Coast, Australia

*Corresponding author: Room 361, Level 3, Building 8, School of Biological Sciences, University of Queensland, St Lucia 4072; Email: r.wheatley@uq.edu.au

Key-words:

trade-off, performance, manoeuvrability, grip, movement, cornering

Summary Statement

Little is known about how terrain affects an animal's agility. We establish that a low-friction surface reduces agility and decreases the movement speeds chosen by a small marsupial.

ABSTRACT

Movement speed can underpin an animal's probability of success in ecological tasks. Prey often use agility to outmanoeuvre predators, however faster speeds increase inertia and reduce agility. Agility is also constrained by grip, as the foot must have sufficient friction with the ground to apply the forces required for turning. Consequently, ground surface should affect optimum turning speed. We tested the speed-agility trade-off in buff-footed antechinus (*Antechinus mysticus*) on two different surfaces. Antechinus used slower turning speeds over smaller turning radii on both surfaces, as predicted by the speed-agility trade-off. Slipping was 64% more likely on the low-friction surface, and had a higher probability of occurring the faster the antechinus were running before the turn. However, antechinus compensated for differences in surface friction by using slower pre-turn speeds as their amount of experience on the low-friction surface increased, which consequently reduced their probability of slipping. Conversely, on the high-friction surface, antechinus used faster pre-turn speeds in later trials, which had no effect on their probability of slipping. Overall, antechinus used larger turning radii (0.733 ± 0.062 vs 0.576 ± 0.051 m) and slower pre-turn (1.595 ± 0.058 vs 2.174 ± 0.050 ms⁻¹) and turning speeds (1.649 ± 0.061 vs 2.01 ± 0.054 ms⁻¹) on the low-friction surface. Our results demonstrate the interactive effect of surface friction and the speed-agility trade-off on speed choice. To predict wild animals' movement speeds, future studies should examine the interactions between biomechanical trade-offs and terrain, and quantify the costs of motor mistakes in different ecological activities.

INTRODUCTION

An animal's ability to escape from danger is fundamental to its survival. However, until recently, escape performance was mainly studied in the context of top speed, rather than the animal's abilities to outrun and outmanoeuvre pursuers (Irschick et al., 2008; Wilson et al., 2015b). In natural situations, prey species do not simply run in fast straight lines, but accelerate, decelerate, and turn (Alexander, 1982; Howland, 1974), and these behaviours are constrained by biomechanical trade-offs (Wheatley et al., 2015; Wilson et al., 2015b; Wynn et al., 2015). Faster speeds are associated with reduced accuracy or precision of movement (i.e. the speed vs. accuracy trade-off; Fitts, 1992; Jayne et al., 2014), which can cause missteps or slips (Amir Abdul Nasir et al., 2017; Irschick and Losos, 1999; Losos and Sinervo, 1989; Sinervo and Losos, 1991; Wheatley et al., 2015). Faster speeds also increase the inertia required to change direction (i.e. speed vs. agility trade-off; Howland, 1974), which constrains the turning radius an animal can use and still remain stable. Prey species may take advantage of these trade-offs to escape from predators that possess faster top speeds than their own (see Wilson et al., 2013a; Wilson et al., 2013b).

Yet escape performance is not simply a matter of biomechanics; wild animals move through environments that vary in complexity, structure, and substrate. These factors interact with biomechanical trade-offs to further constrain movement. For example, buff-footed antechinus (*Antechinus mysticus*) and northern quolls (*Dasyurus hallucatus*) both moderate their escape speeds when they run across narrow branches to minimise their risk of slips or falls (Amir Abdul Nasir et al., 2017; Wheatley et al., 2018). Narrow branches offer a smaller target for foot placement, and slower speeds increase the accuracy of footing because speed and accuracy act in opposition to one another.

Ultimately, we expect animals to moderate their speeds relative to biomechanical (i.e. speed versus agility) and environmental (i.e. branch width) constraints. Substrate is an important environmental factor affecting movement. Coarse or rough surfaces can often increase friction between the foot and the ground, and consequently increase the animal's potential acceleration, deceleration, and straight and angular running speeds (Alexander, 1982; Brandt et al., 2015; Brechue et al., 2005; Höfling et al., 2012). In contrast, smooth, low-friction surfaces reduce the animal's ability to apply the appropriate forces for fast forward or turning movement (van der Tol et al., 2005), and it must slow down to avoid slipping. Friction is so important to animal movement that many species have evolved specialised foot pads or claws to augment their purchase on the ground (Alexander, 2002; Cartmill, 1979). Although studies on lizards recorded faster straight running speeds on substrates that allowed increased friction (Brandt et al., 2015; Höfling et al., 2012; Vanhooydonck et al., 2015), to our knowledge, no studies have compared other performance traits across substrates that vary in surface friction.

We tested how ground substrate affects the trade-off between speed and agility in a small marsupial, the buff-footed antechinus (*Antechinus mysticus* Baker, Mutton & Van Dyck, 2012). Buff-footed antechinus are mouse-sized (20 – 50 g) insectivorous marsupials (Mutton et al., 2017) that forage on both high- and low-friction surfaces: in leaf litter and bark on the ground, on fallen timber, and on tree trunks including smooth-barked Eucalypts (Dickman, 1980; Fisher and Dickman, 1993). They have numerous enlarged, striated pads on their fore- and hind-feet and large claws to assist with grip (Baker et al., 2012). We encouraged antechinus to run and turn on surfaces that differed in their frictional properties, and predicted that they would slip more frequently when attempting to complete sharp turns at higher speeds, and on a smooth, low-friction surface. We demonstrate that, in addition to biomechanical trade-offs between speed and agility, antechinus behaviourally compensate for surface friction by reducing their speed and making wider turns on the low-friction surface.

MATERIALS AND METHODS

Animal collection and husbandry

We collected eighteen adult female buff-footed antechinus (*Antechinus mysticus*) from the Great Sandy National Park on the Fraser Coast, Queensland from June through September 2014, in accordance with a Queensland Government's Department of Environment and Heritage Protection permit (DEHP permit number: WITK14120114). Antechinus were captured in waterproofed (Biopak compostable bags) Elliot traps lined with Dacron fibre and baited with peanut butter, oats, and minced beef. All animals were micro-chipped (ID-100A(1.25) Nano Transponder, Trovan Unique, United Kingdom) and treated for parasites (animal mite and mange spray, Aristopet, Brisbane, Australia) before being transported back to Brisbane, where they were housed in custom-built enclosures (3 × 3 × 2 m) in groups of three individuals. Each enclosure was fitted with pine bark chip substrate (Nudgee Road Landscape Supplies, Brisbane, Australia), three wooden nest boxes, three mouse running wheels, and a wooden climbing frame. Animals were provided with a constant water source (250 mL inverted drip water bottles, Kazoo, Lidcombe, Australia), and were fed daily with a mixture of minced meat, crushed dog kibble, egg powder, small animal vitamin drops (Aristopet, Brisbane, Australia) and a calcium carbonate powder supplement. This was supplemented with live invertebrates every alternate day. All experiments were performed in accordance with the animal use in research ethics protocol approved by the University of Queensland's Animal Ethics Committee (AEC approval number: SBS/397/13/ARC).

Cornering performance on two surfaces

Experiments were conducted in a $3 \times 3 \times 2$ m outdoor enclosure. Inside the enclosure was a $1.0 \times 0.2 \times 0.6$ m runway constructed using medium density fibreboard walls (9 mm, Customwood, Daiken, New Zealand) and a rough concrete floor. One end of the runway opened out into a 1.5×1.5 m clear arena, with an open, empty Elliot trap in every corner which the antechinus used as a refuge (Fig. 1). The ground substrate of the arena was either a high- (rough concrete) or low-friction (smooth corrugated plastic; white Corflute, Bunnings Warehouse, Brisbane, Australia) surface. Neither surface was soft enough for the antechinus' claws to puncture or indent. The arena was illuminated using Tobi clamp lamps (Verve design), while the interiors of the track and Elliot traps were dark.

We used mass as the most accurate measure of overall size for all of the animals in our study (mean = 30.95 ± 0.72 g), however some additional linear measurements of size are provided for a subset of the antechinus in the supplementary material (Table S1). Each antechinus had a 2×2 cm marker (a square of masking tape with a 0.5 cm diameter circle drawn in black pen at the centre) affixed to its back to aid in frame-by-frame analyses of video footage. During the trial, an individual antechinus was placed at the closed end of the runway and encouraged to run down the runway into the arena by a researcher shaking a plastic bag behind them. Another researcher stood (immobile) along the wall across from the open end of the runway (Fig. 1) to passively encourage turning. Turning behaviour in the open arena was filmed using a high-speed camera (Casio Exilim EX-FH25, Tokyo, Japan) at 240 fps from directly above at the point where the runway met the arena. The dimensions of the resulting videos were 448×336 pixels and 1.35×1.1 m. Each antechinus performed ten trials on each surface, with a 10 minute break between trials to prevent fatigue. Trials where the antechinus did not run continuously were discarded, as were runs where the turning radius exceeded 2 m

(as only eight of these turns were made across both surfaces, and for an animal of that size over such a short distance, such “turns” were essentially straight lines).

Data were extracted from the video footage following a procedure modified from Wynn et al. (2015). The position of the marker on each antechinus’ back was tracked into and through the turn (where a turn was defined by a $>15^\circ$ change in the antechinus’ trajectory) using Tracker video analysing software (Version 4.87, Open Source Physics, Boston, USA). These positions were then smoothed by a mean squared error algorithm (TOL = 0.05 error in pixels/frame) using a custom-written script in MATLAB (R2016b, Mathworks; available upon request from the corresponding author), and the following data extracted: (1) pre-turn speed (ms^{-1}), the mean of all instantaneous velocities in the stride immediately preceding the start of the turn, where the change in trajectory was $\leq 15^\circ$; (2) turning speed (ms^{-1}), the mean of all instantaneous velocities throughout the turn; (3) turning radius (m), determined by a circle fitted to the antechinus’ positional data around the turn using the least squares modelling approach outlined in Pratt (1987); and (4) turning angle ($^\circ$), the total absolute change in the antechinus’ trajectory through the turn. We also quantified both the number of strides within the turn, and the number of slips (by counting the number of strides where the antechinus failed to gain purchase on the surface, causing its legs to slip out from under it). From this, we calculated the proportion of turning strides containing a slip for each trial.

To determine how friction limited turning speed, we evaluated eight different friction limit models against turns where no slips occurred on each surface. The minimum coefficient of friction required to execute a turn of a particular radius at a given speed without slipping was estimated by Alexander (1982) as $\mu = V^2/rg$, where V is the turning speed, r is the turning radius, and g is acceleration due to gravity. Using this equation, we generated eight different potential models for the relationship between turning speed and turning radius up to 0.5 m using friction coefficients of 0.7 – 1.4. We determined which of these eight models best fit the

experimental data for each surface using the method described in Tan and Wilson (2011). First, the experimental turning speed data for turns ≤ 0.5 m in radius where no slips occurred were grouped according to turning radius into categories of 0.05 m (i.e. turning speeds for $0 < r \leq 0.05$ m, turning speeds for $0.05 < r \leq 0.1$, etc.). The 99th turning speed percentile (i.e. the 99% point of the turning speed) was calculated for each data group. Next, we calculated the turning speed values predicted by each friction limit model for the upper turning radius of each category (i.e. 0.05 m, 0.1 m, etc.). The error of each friction limit model was taken as the difference between the 99% turning speed percentiles and the turning speed values predicted by the model, and was expressed as a percentage of the experimental data. The best model was the one with the smallest error, and the friction coefficient from this model was taken as the minimum coefficient of friction for that surface. The correlation between the best model and the 99% percentiles was calculated using Pearson's product-moment correlation.

Statistical analyses

Data analyses were conducted in the R statistical software environment version 3.4.0 (R Foundation for Statistical Computing, Vienna, Austria). A linear mixed effects regression model (LMM) was fitted to the pre-turn speed data using the *nlme* v3.1.128 package (Pinheiro et al., 2017) with the effects of surface friction, shelter orientation (backward or forward), mass, trial number, and their two-way interactions as fixed effects and individual as a random effect. Statistically significant correlations were determined using ANOVA, and were used as interaction terms in subsequent models.

Linear mixed effects regression models were fitted to determine the effects of surface friction, shelter orientation, mass, trial number, pre-turn speed, turning radius, turning speed, turning angle, the proportion of turning strides with a slip (where a slip did occur), and their various interactions on one another. Where turning radius or turning speed was the response variable, \ln transformations were used on all continuous variables to satisfy the assumption of linearity. The proportion of turning strides with a slip was *arcsine square root* transformed to satisfy the assumption of normality. Generalized linear mixed effects regression models (GLMM) with binomial distributions were fitted using the *lme4* v1.1.0 package (Bates et al., 2015) to determine the effects of surface friction, shelter orientation, mass, pre-turn speed, turning radius, turning speed, turning angle, and their various interactions on the presence of a slip. In all cases, individual was a random effect. All full models were simplified using conditional model averages through the *MuMIn* v1.15.6 package (Barton 2016), using Akaike weights of ≥ 0.01 to subset the model. Near-zero importance models were then removed by fitting a cumulative sum of Akaike weights to ≤ 0.995 . Full tables of averaged models are presented in the supplementary material (Table S2 – S6).

RESULTS

Antechinus used ~36% faster pre-turn speeds on the high-friction surface than the low-friction surface (2.174 ± 0.050 vs 1.595 ± 0.058 ms^{-1} , $n = 151$, $F_{1,129} = 72.259$, $P < 0.0001$); this was because *antechinus* altered their choice of movement speed with trial number ($n = 151$, $F_{1,129} = 7.154$, $P = 0.008$). *Antechinus* used faster pre-turn speeds with experience on the high-friction surface ($n = 83$, $F_{1,63} = 5.212$, $P = 0.026$; Fig. 2), but used slower pre-turn speeds with experience on the low-friction surface ($n = 68$, $F_{1,49} = 4.795$, $P = 0.033$; Fig. 2).

Turning radius was positively associated with both pre-turn speed (Table 1; Fig. 3A) and turning speed (Table 2; Fig. 3B). Although the relationship between pre-turn speed and surface friction did not significantly affect turning radius, antechinus turned with greater radii on the low-friction surface (0.733 ± 0.062 vs 0.576 ± 0.051 m; Table 1). Neither pre-turn speed ($n = 151$, $F_{1, 16} = 3.403$, $P = 0.084$) nor turning radius (Table 1) was associated with body mass, and turning radius did not change with trial number as trial was not present in any of the averaged models (Table S2).

Antechinus that had faster pre-turn speeds also turned using faster speeds across both surfaces (Table 2). Turning speeds were significantly faster on the high-friction surface (2.01 ± 0.054 vs 1.649 ± 0.061 ms^{-1} ; Table 2), and the plateau occurred at a 25% faster speed (~ 2.5 vs 2.0 m s^{-1}). Turning speed was not associated with body mass (Table 2) or trial number (trial was not present in the averaged models; Table S3).

For the combined data for the two surfaces, antechinus were $\sim 64\%$ more likely to slip (lose their footing) when turning on the low-friction surface ($n = 151$, $Z = 5.269$, $P < 0.0001$), but this changed depending on the number of trials performed on each surface ($n = 151$, $Z = -2.762$, $P = 0.006$). Antechinus improved with experience and were less likely to slip in later trials on the low-friction surface ($n = 68$, $Z = -2.752$, $P = 0.006$; Fig. 4A). However, trial number did not affect the probability of slipping on the high-friction surface ($n = 83$, $Z = 1.208$, $P = 0.227$; Fig. 4A). Slips were more likely at higher pre-turn speeds ($n = 151$, $Z = 2.927$, $P = 0.003$; Fig. 4B), but at slower turning speeds ($n = 151$, $Z = -3.622$, $P < 0.0003$; Fig. 4C). Slips were not associated with turning angle, turning radius, or body mass (neither turning angle, turning radius nor body mass were present in the only model with a weight of > 0.01 ; Table S4).

If the antechinus slipped, they tended to be more likely to slip multiple times during the same trial on the low-friction versus the high-friction surface (0.545 ± 0.047 vs 0.073 ± 0.022 turning strides with a slip; Table 3). However, the proportion of strides with a slip during the turn (if they slipped at all) was not associated with turning speed, turning radius, pre-turn speed, or trial number (Table 3), nor turning angle or body mass (neither turning angle nor body mass were present in the averaged models; Table S5).

Antechinus turned through greater angles when heading toward the backward oriented shelters (Table 4). Turning angle was independent of turning speed, turning radius, pre-turn speed, surface friction, mass and trial number (Table 4), and had no effect on the probability of slipping ($n = 151$, $Z = 0.868$, $P = 0.386$) or the proportion of turning strides with a slip (if a slip occurred; $n = 151$, $Z = 0.082$, $P = 0.935$).

Antechinus heading toward the backward oriented shelters used slower pre-turn speeds ($n = 151$, $F_{1,129} = 33.460$, $P < 0.0001$) and turned with smaller radii ($n = 151$, $Z = 2.811$, $P = 0.005$). Shelter orientation had no effect on turning speed ($n = 151$, $Z = 0.058$, $P = 0.954$), the presence of a slip ($n = 151$, $Z = 1.029$, $P = 0.304$), nor the percent of turning strides with a slip ($n = 67$, $Z = 0.082$, $P = 0.935$). 77% of turns were toward the forward oriented shelters while 23% were toward the backward oriented shelters.

For the high-friction surface, the friction limit model with the lowest error (15.8%) when compared to the real data had a friction coefficient of 1.3 ($R = 0.595$, $t_7 = 1.958$, $P = 0.091$; Table 5, Fig. 5A). For the low-friction surface, the friction limit model with the lowest error (26.3%) assumed a friction coefficient of 0.8 ($R = -0.337$, $t_1 = -0.357$, $P = 0.782$; Table 5, Fig. 5B).

DISCUSSION

Antechinus selected movement speeds based on both the biomechanical trade-off between speed and agility and the probability of slipping on surfaces with different frictional properties. Antechinus chose moderate speeds when entering an unfamiliar environment and then adjusted these speeds over subsequent trials depending on whether the experimental surface was high- or low-friction. Antechinus used similar pre-turn speeds during the first trials on each surface; however, they employed slower pre-turn speeds on subsequent low-friction trials, which reduced the number of slips they made when turning. Antechinus were twice as likely to slip when turning on the low-friction surface as the high-friction surface because—as shown by our friction limit models—their grip on the low-friction surface was nearly half that of the high-friction surface. On the high-friction surface, antechinus used faster pre-turn speeds in later trials, but this did not make them more or less likely to slip when turning.

Lizards run faster on high-friction surfaces (Brandt et al., 2015; Höfling et al., 2012; Vanhooydonck et al., 2015), but our results suggest that variation in straight-running speeds over different surfaces may be due in part to choices made by the animals rather than biomechanical constraints. The risk and cost of motor mistakes are likely to be important in speed choice, particularly during predator pursuits. Antechinus were 64% more likely to lose their footing on the low-friction surface, but the 36% decrease in speed we observed when antechinus ran onto a low-friction surface may also reduce their ability to escape predators. Antechinus were also more likely to slip when they used faster pre-turn speeds on either surface. This is likely due to the antechinus' attempting to apply forces larger than their friction with the substrate permits (van der Tol et al., 2005), resulting in a slip. In contrast, antechinus appeared less likely to slip when using faster turning speeds. Slipping reduced movement speeds considerably, as the antechinus struggled to gain enough purchase to run, so it is likely

the presence of slips during a turn would drag mean turning speed down. Therefore, the negative relationship between turning speed and the probability of slipping may be due to turns that had no slips subsequently having faster mean speeds. Despite being an important cost of high-speed movement, no studies to date have examined slipping or other motor mistakes and their consequences on fitness. However, in order to accurately predict the movement speeds animals choose, we must understand the costs of motor mistakes.

Overall, antechinus used slower turning speeds when making tighter turns, suggesting that the trade-off between speed and agility constrains turning radius (Howland, 1974). Although stability is a strong driver for reducing speed (Full et al., 2002; Ting et al., 1994), the turning speeds of terrestrial animals are constrained by the forces that the limbs can withstand (Wilson et al., 2015a). When turning, these forces are gravity and those associated with centripetal acceleration (Usherwood and Wilson, 2006). The more sharply an animal turns, the greater the centripetal forces it experiences. Many animals compensate for this by increasing the proportion of the stride where their feet are in contact with the ground (the duty factor) on sharp turns (Chang and Kram, 2007; Greene, 1987; Usherwood and Wilson, 2006; Walter, 2003). This increase in duty factor can decrease movement speed if other stride parameters do not change (Greene and McMahon, 1979). Wild mice (*Mus musculus*) used this mechanism to reduce their speed when making 90° turns (Walter, 2003). Consequently, the speed-agility trade-off we observe may be due to a combination of reduced stability and increasing limb forces at higher turning speeds.

Across surfaces, when antechinus used slower pre-turn speeds, they subsequently made tighter, slower turns. However, on the low-friction surface, antechinus tended to use slower pre-turn speeds *and* make wider turns. Antechinus selected pre-turn speeds based on the expected friction of the surface, but their turning speeds and radii were also constrained by friction. Both our results and the friction limit models predict that agility (or turning radius)

should improve with increased friction. However, turning speed at any given turning radius is *also* constrained by the maximum speed the animal can run. At small turning radii, where animals must use slower speeds to remain stable, speed is primarily limited by friction (Alexander, 2002; Tan and Wilson, 2011). As turning radius increases, speed becomes limited by the force the animal is capable of driving into the ground (Weyand et al., 2000). Thus, agility is only constrained by friction alone at small turning radii, and consequently friction limit models will only provide an accurate estimate of turning speeds at these small radii (Tan and Wilson, 2011). It is also essential to note that increasing surface friction will only improve friction between the foot and the ground (and therefore agility) to a certain extent. Particularly for small species such as antechinus, extremely uneven surfaces will require greater precision of foot placement to avoid tripping, which may in turn require slower movement speeds. The smooth and rough flooring we used in our experiment was intended to encompass natural variation in smoothness of tree bark and rocks these semi-arboreal animals would experience in the wild (Dickman, 1980; Fisher and Dickman, 1993), but future studies could expand our work by using natural surfaces.

We have assumed that turning ability is constrained by friction at every point during the turn. However, antechinus employed a bounding quadrupedal gait on both surfaces across all trials, and consequently, there was a phase during each stride where no feet were in contact with the substrate. Our antechinus had relatively long tails proportional to body length (83.80 ± 1.17 vs 64.09 ± 1.02 mm), and were observed swinging their tails considerably during turns. Kangaroo rats (*Dipodomys* spp.) can turn while their feet are off the ground by rapidly moving their tail (Bartholomew and Caswell, 1951). Using a similar method, antechinus may be able to turn during the stride phase where their feet are not in contact with the substrate, thus overcoming the limitations to speed imposed by friction. This may explain why 51% and 40% of the turns were faster than those predicted by the best friction limit models on the high- and

low-friction surfaces. However, due to the limited number of turns where no slips occurred, particularly on the low-friction surface, the predicted turning speed values from the best friction limit models are not significantly correlated with the real turning speed data. Consequently, our estimates for the coefficient of friction on each surface are highly approximate.

Our study supports a growing body of evidence showing that animals select running speeds based on biomechanical trade-offs (Amir Abdul Nasir et al., 2017; Losos and Sinervo, 1989; Sinervo and Losos, 1991; Wilson et al., 2013a; Wheatley et al., 2018; Wynn et al., 2015) and the terrain over which they are moving (Amir Abdul Nasir et al., 2017; Losos and Sinervo, 1989; Sinervo and Losos, 1991; Vanhooydonck et al., 2015; Wheatley et al., 2018). It is important that researchers both consider and report on the surface structure and friction in their studies, and because the effects of friction will differ among species with different kinds of feet (Höfling et al., 2012), a metric of friction that pairs species and substrate would be ideal. This could be something as simple as the coefficient of friction estimated from friction limit models. *Antechinus* also modified their speeds depending on how likely they were to slip across surfaces. Future research should work toward quantifying the costs of motor mistakes such as slipping in different ecological activities (such as foraging or escaping from a predator) or habitats. Understanding the combined effects of biomechanical trade-offs, terrain, and the probability of mistakes on fitness is essential to predicting animal movement speeds in the wild.

ACKNOWLEDGEMENTS

This work would not have been possible without our many undergraduate students and volunteers, who assisted with antechinus trapping and husbandry. We would also like to thank Thomas Mutton and Andrew Baker for genetically confirming the study species, Daniella Parra for providing advice regarding trapping and husbandry, Maya Maia and Nora Allen for their help with data collection, Simon Blomberg for his advice on our statistical analyses, Gwendolyn David for helping construct our figures, and two anonymous reviewers for their detailed and thoughtful suggestions.

COMPETING INTERESTS

No competing interests declared for all authors.

FUNDING

This work was supported by the Australian Research Council [DE130101410 to A.C.N., DP150100198 to R.S.W. and D.O.F., FT150100492 to R.S.W], the Holsworth Wildlife Research Endowment [to R.W.], and the Ecological Society of Australia [to R.W.].

DATA AVAILABILITY

Data will be uploaded to Dryad upon manuscript acceptance.

REFERENCES

- Alexander, R. M.** (1982). *Locomotion of animals*. Glasgow: Blackie.
- Alexander, R. M.** (2002). Stability and manoeuvrability of terrestrial vertebrates. *Integrative and Comparative Biology* **42**, 158–164.
- Amir Abdul Nasir, A. F., Clemente, C. J., Wynn, M. L. and Wilson, R. S.** (2017). Optimal running speeds when there is a trade-off between speed and the probability of mistakes. *Functional Ecology* **31**, 1941–1949.
- Baker, A. M., Mutton, T. Y. and Van Dyck, S.** (2012). A new dasyurid marsupial from eastern Queensland, Australia: the buff-footed antechinus, *Antechinus mysticus* sp nov (Marsupialia: Dasyuridae). *Zootaxa* **3515**, 1–37.
- Bartholomew, G. A. and Caswell, H. H.** (1951). Locomotion in kangaroo rats and its adaptive significance. *Journal of Mammology* **32**, 155–169.
- Barton, K.** (2016). MuMIn: multi-model inference. R package version 1.15.6, <https://CRAN.R-project.org/package=MuMIn>.
- Bates, D., Maechler, M., Bolker, B., & Walker, S.** (2015). Fitting linear mixed-effects models using lme4. *Journal of Statistical Software* **67**, 1–48.
- Brandt, R., Galvani, F. and Kohlsdorf, T.** (2015). Sprint performance of a generalist lizard running on different substrates: grip matters. *Journal of Zoology* **297**, 15–21.
- Brechue, W. F., Mayhew, J. L. and Piper, F. C.** (2005). Equipment and running surface alter sprint performance of college football players. *Journal of Strength and Conditioning Research* **19**, 821–825.
- Cartmill, M.** (1979). The volar skin of primates: its functional characteristics and their functional significance. *American Journal of Physical Anthropology* **50**, 497–510.
- Chang, Y. H. and Kram, R.** (2007). Limitations to maximum running speed on flat curves. *Journal of Experimental Biology* **210**, 971–982.

Dickman, C. (1980). Ecological studies of *Antechinus stuartii* and *Antechinus flavipes* (Marsupialia: Dasyuridae) in open-forest and woodland habitats. *Australian Zoologist* **20**, 433–446.

Fisher, D. O. and Dickman, C. R. (1993). Body size-prey relationships in insectivorous marsupials: tests of three hypotheses. *Ecology* **74**, 1871–1883.

Fitts, P. M. (1992). The information capacity of the human motor system in controlling the amplitude of movement (reprinted from *Journal of Experimental Psychology*, vol 47, pg 381-391, 1954). *Journal of Experimental Psychology General* **121**, 262–269.

Full, R. J., Kubow, T., Schmitt, J., Holmes, P. and Koditschek, D. (2002). Quantifying dynamic stability and maneuverability in legged locomotion. *Integrative and Comparative Biology* **42**, 149–157.

Greene, P. R. (1987). Sprinting with banked turns. *Journal of Biomechanics* **20**, 667–680.

Greene, P. R. and McMahon, T. A. (1979). Running in circles. *The Physiologist* **22**, S35–6.

Höfling, E., Renous, S., Curcio, F. F., Eterovic, A. and Santos Filho, P. d. S. (2012). Effects of surface roughness on the locomotion of a long-tailed lizard, *Colobodactylus taunayi* Amaral, 1933 (Gymnophthalmidae: Heterodactylini). *International Journal of Zoology* **2012**, 16 pages.

Howland, H. C. (1974). Optimal strategies for predator avoidance - relative importance of speed and maneuverability. *Journal of Theoretical Biology* **47**, 333–350.

Irschick, D. J. and Losos, J. B. (1999). Do lizards avoid habitats in which performance is submaximal? The relationship between sprinting capabilities and structural habitat use in Caribbean anoles. *The American Naturalist* **154**, 293–305.

Irschick, D. J., Meyers, J. J., Husak, J. F. and Le Galliard, J. F. (2008). How does selection operate on whole-organism functional performance capacities? A review and synthesis. *Evolutionary Ecology Research* **10**, 177–196.

Jayne, B. C., Lehmkuhl, A. M. and Riley, M. A. (2014). Hit or miss: branch structure affects perch choice, behaviour, distance and accuracy of brown tree snakes bridging gaps. *Animal Behaviour* **88**, 233–241.

Losos, J. B. and Sinervo, B. (1989). The effects of morphology and perch diameter on sprint performance of *Anolis* lizards. *Journal of Experimental Biology* **145**, 23–30.

Mutton, T. Y., Gray, E. L., Fuller, S. J. and Baker, A. M. (2017). Life history, breeding biology and movement in a new species of carnivorous marsupial, the buff-footed antechinus (*Antechinus mysticus*) and a sympatric congener, the subtropical antechinus (*Antechinus subtropicus*). *Mammal Research* **62**, 373–385.

Pinheiro, J., Bates, D., DebRoy, S., Sarkar, D., & R Core Team. (2017). nlme: linear and nonlinear mixed effects models. R package version 3.1-131, <https://CRAN.R-project.org/package=nlme>.

Pratt, V. (1987). Direct least-squares fitting of algebraic surfaces. *ACM SIGGRAPH Computer Graphics* **21**, 145–152.

Sinervo, B. and Losos, J. B. (1991). Walking the tight rope - arboreal sprint performance among *Sceloporus occidentalis* lizard populations. *Ecology* **72**, 1225–1233.

Tan, H. L. and Wilson, A. M. (2011). Grip and limb force limits to turning performance in competition horses. *Proceedings of the Royal Society B-Biological Sciences* **278**, 2105–2111.

Ting, L. H., Blickhan, R. and Full, R. J. (1994). Dynamic and static stability in hexapedal runners. *Journal of Experimental Biology* **197**, 251–269.

Usherwood, J. R. and Wilson, A. M. (2006). Accounting for elite indoor 200 m sprint results. *Biology Letters* **2**, 47–50.

van der Tol, P. P. J., Metz, J. H. M., Noordhuizen-Stassen, E. N., Back, W., Braam, C. R. and Weijs, W. A. (2005). Frictional forces required for unrestrained locomotion in dairy cattle. *Journal of Dairy Science* **88**, 615–624.

Vanhooydonck, B., Measey, J., Edwards, S., Makhubo, B., Tolley, K. A. and Herrel, A. (2015). The effects of substratum on locomotor performance in lacertid lizards. *Biological Journal of the Linnean Society* **115**, 869–881.

Walter, R. M. (2003). Kinematics of 90° running turns in wild mice. *Journal of Experimental Biology* **206**, 1739–1749.

Weyand, P. G., Sternlight, D. B., Bellizzi, M. J. and Wright, S. (2000). Faster top running speeds are achieved with greater ground forces not more rapid leg movements. *Journal of Applied Physiology* **89**, 1991–1999.

Wheatley, R., Angilletta, M. J., Jr., Niehaus, A. C. and Wilson, R. S. (2015). How fast should an animal run when escaping? An optimality model based on the trade-off between speed and accuracy. *Integrative and Comparative Biology* **55**, 1166–1175.

Wheatley, R., Niehaus, A. C., Fisher, D. O. and Wilson, R. S. (2018). Ecological context and the probability of mistakes underlie speed choice. *Functional Ecology* **00**, 1–11.

Wilson, A. M., Lowe, J. C., Roskilly, K., Hudson, P. E., Golabek, K. A. and McNutt, J. W. (2013a). Locomotion dynamics of hunting in wild cheetahs. *Nature* **498**, 185–189.

Wilson, J. W., Mills, M. G., Wilson, R. P., Peters, G., Mills, M. E., Speakman, J. R., Durant, S. M., Bennett, N. C., Marks, N. J. and Scantlebury, M. (2013b). Cheetahs, *Acinonyx jubatus*, balance turn capacity with pace when chasing prey. *Biology Letters* **9**, 20130620.

Wilson, R. P., Griffiths, I. W., Mills, M. G. L., Carbone, C., Wilson, J. W. and Scantlebury, D. M. (2015a). Mass enhances speed but diminishes turn capacity in terrestrial pursuit predators. *eLife* **4**, 18 pages.

Wilson, R. S., Husak, J. F., Halsey, L. G. and Clemente, C. J. (2015b). Predicting the movement speeds of animals in natural environments. *Integrative and Comparative Biology* **55**, 1125–1141.

Wynn, M. L., Clemente, C., Nasir, A. F. A. A. and Wilson, R. S. (2015). Running faster causes disaster: trade-offs between speed, manoeuvrability and motor control when running around corners in northern quolls (*Dasyurus hallucatus*). *Journal of Experimental Biology* **218**, 433–439.

Figures

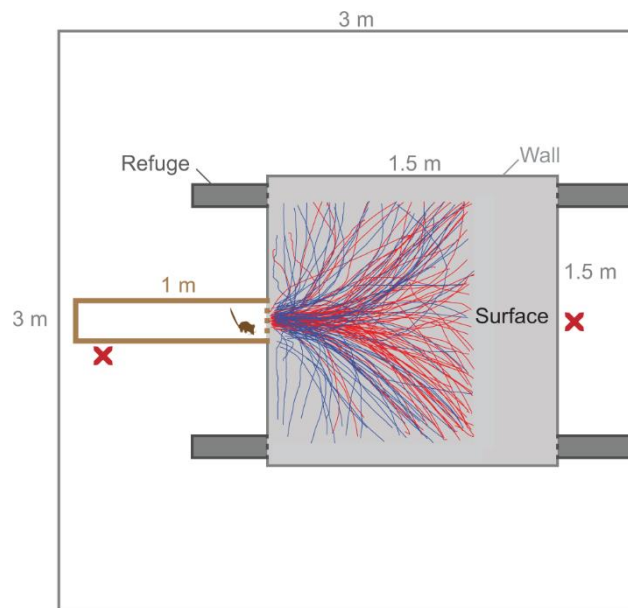


Fig. 1. Top view of the running track and arena construction showing antechinus' unsmoothed turning paths. The set up was contained inside a $3 \times 3 \times 2$ m outdoor enclosure. Walls were 0.6 m high and made from 9 mm medium density fibreboard. The set up consisted of a 1 m running track with a concrete surface, which opened out into a 1.5×1.5 m illuminated arena (grey area) with an open Elliot trap in each corner. The surface of the arena was either rough concrete (high-friction), or white Corflute (low-friction). An experimenter was positioned at each red cross. Antechinus were filmed from above at the point where the running track opens into the arena. Unsmoothed turning paths within the camera's field of view are shown for the high-friction (red) and low-friction (blue) surfaces.

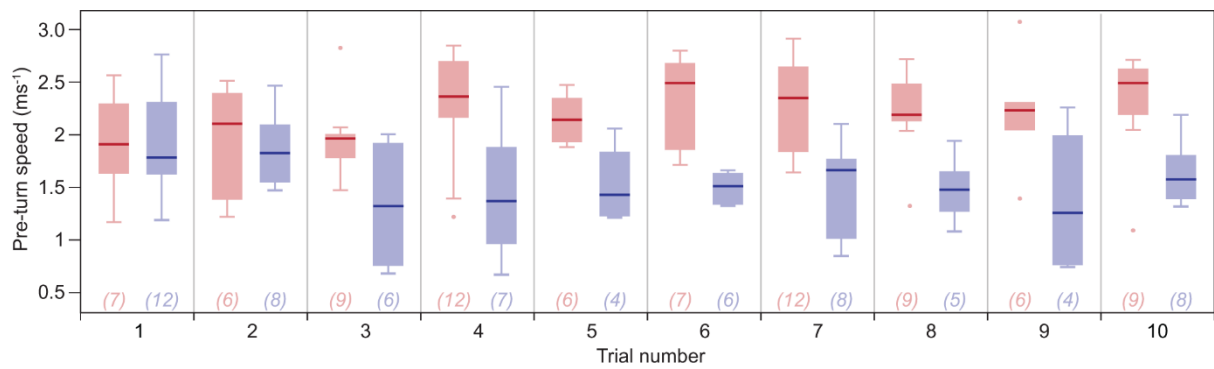


Fig. 2. Relationship between pre-turn speed and trial number for each surface friction.

Blue represents the low-friction surface, while red represents the high-friction surface. Antechinus used faster pre-turn speeds with increasing trial numbers on the high-friction surface, but slower pre-turn speeds on the low-friction surface. Boxes represent the 1st quartile, median, and 3rd quartile, while whiskers represent the 95% confidence interval. Sample sizes are shown in parentheses beneath each plot.

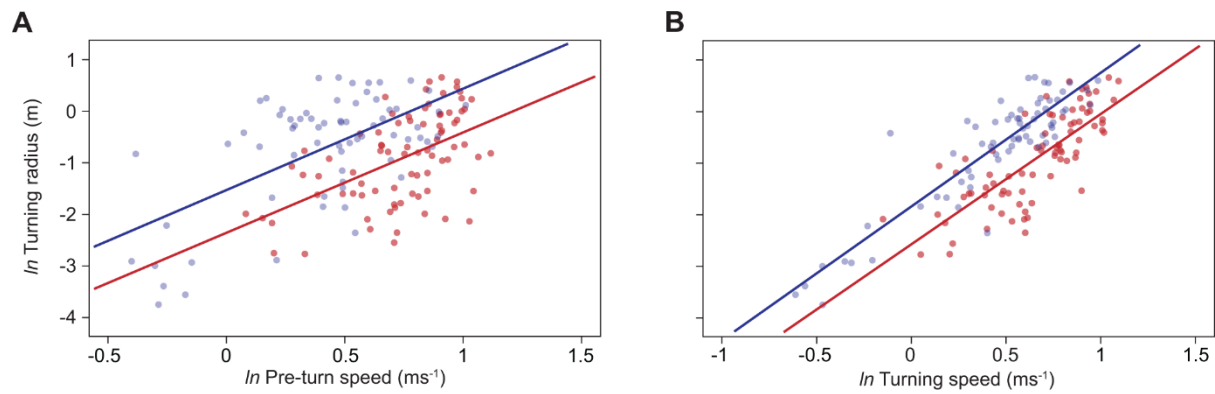


Fig. 3. Relationship between \ln turning radius and \ln pre-turn speed (A), and \ln turning speed (B). Blue represents the low-friction surface, while red represents the high-friction surface. Solid lines represent the linear regression models fitted to the data, while circles represent the raw data. Turning radius increased with both (A) pre-turn speed and (B) turning speed.

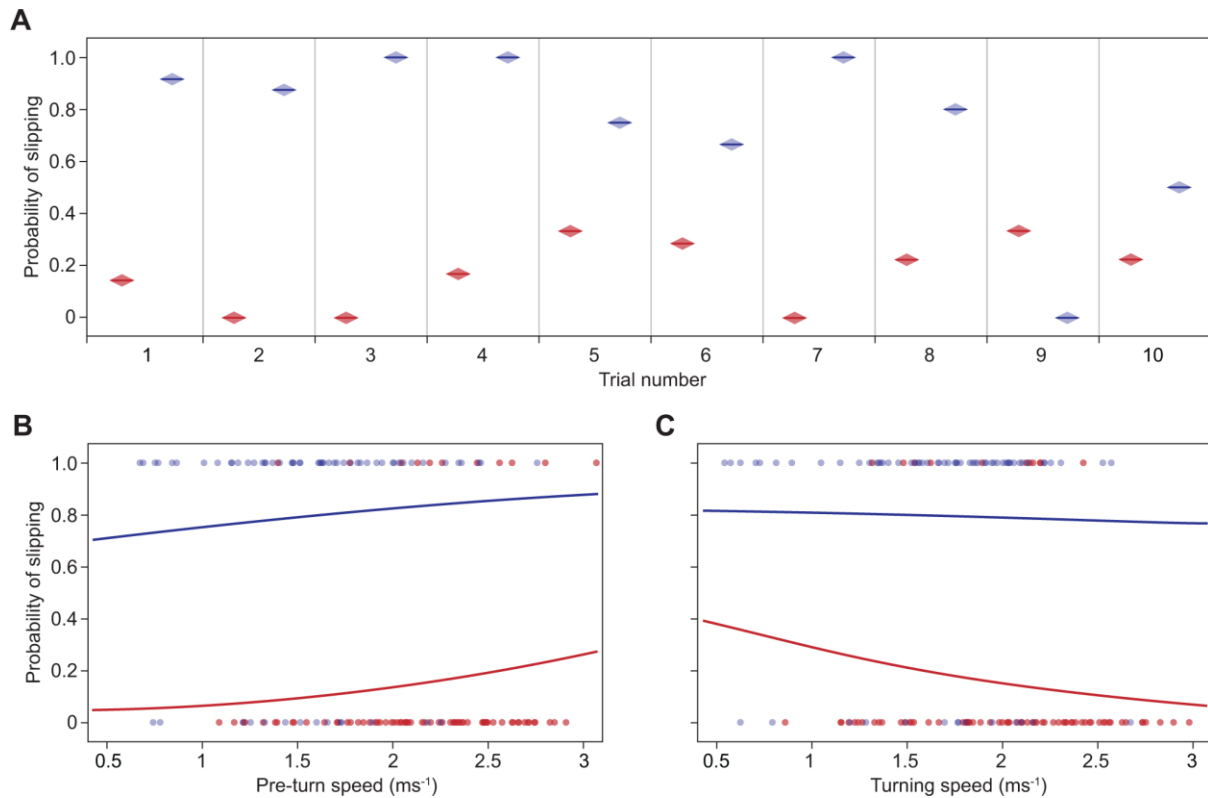


Fig. 4. Effect of trial number (A), pre-turn speed (B), and turning speed (C) on the probability of slipping when turning. Blue represents the low-friction surface ($n = 68$), while red represents the high-friction surface ($n = 83$). (A) The probability of slipping decreased with trial number on the low-friction surface, but trial number had no effect on the probability of slipping on the high-friction surface. Across trials, slipping when turning was more likely on the low-friction surface, and when the antechinus used higher pre-turning speeds (B) and lower turning speeds (C). Solid lines represent the binomial regression fitted to the data, while circles represent the raw data.

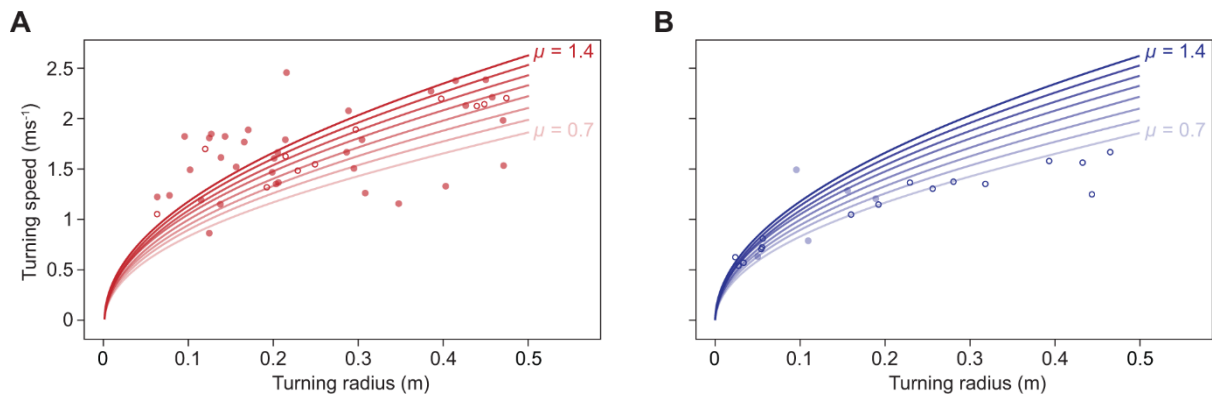


Fig. 5. Relationship between turning speed and turning radius for the high-friction (A) and low-friction (B) surfaces, where turning radius ≤ 0.5 m. Turning radius was significantly correlated with turning speed. Blue represents the low-friction surface ($n = 68$), while red represents the high-friction surface ($n = 83$). Solid lines represent the relationship predicted by the friction limit models, with coefficients (μ) of 0.7, 0.8, 0.9, 1.0, 1.1, 1.2, 1.3, and 1.4 represented by the progressively darker shades. Filled circles represent the data points where a slip did not occur, while open circles represent the data points where a slip did occur. The best fitting friction limit models have a friction coefficient of 1.3 for the high-friction surface, and 0.8 for the low-friction surface.

Tables

Table 1. Full output of model-averaged LMMs predicting \ln turning radius ($n = 151$).

Response: \ln turning radius	Estimate	Standard Error	z value	P value	Importance
(Intercept)	-0.951	2.363	0.402	0.687	
\ln pre-turn speed	1.684	0.387	4.351	1E-5*	1.00
friction	1.405	0.466	3.012	0.003*	1.00
shelter orientation	-1.124	0.400	2.811	0.005*	1.00
\ln mass	-0.333	0.727	0.458	0.647	0.49
\ln pre-turn speed · friction	-0.867	0.715	1.213	0.225	0.75
\ln pre-turn speed · shelter orientation	1.154	0.726	1.589	0.112	0.86

The full model contained \ln turning radius as the response variable, \ln pre-turn speed, surface friction, shelter orientation, \ln mass, trial number, the interactions between \ln pre-turn speed and surface friction, \ln pre-turn speed and shelter orientation, and surface friction and trial number as fixed effects, and individual as a random effect. All continuous variables were \ln transformed to satisfy the assumption of linearity. Only variables present in at least one of the averaged models (importance > 0) are reported in the table.

Table 2. Full output of model-averaged LMMs to predict *ln* turning speed (*n* = 151).

Response: <i>ln</i> turning speed	Estimate	Standard Error	<i>z</i> value	<i>P</i> value	Importance
(intercept)	0.487	0.123	3.958	8E-6*	
<i>ln</i> turning radius	0.203	0.015	13.518	2E-16*	1.00
<i>ln</i> pre-turn speed	0.464	0.054	8.649	2E-16*	1.00
friction	-0.104	0.036	2.898	0.004*	0.97
shelter orientation	5E-4	0.009	0.051	0.959	0.04
<i>ln</i> mass	0.002	0.035	0.056	0.955	0.07
<i>ln</i> turning radius · <i>ln</i> pre-turn speed	-0.002	0.010	0.187	0.851	0.05
<i>ln</i> turning radius · shelter orientation	9E-4	0.008	0.112	0.911	0.01
<i>ln</i> pre-turn speed · friction	0.004	0.026	0.169	0.866	0.07

The full model contained *ln* turning speed as the response variable, *ln* turning radius, *ln* pre-turn speed, surface friction, shelter orientation, *ln* mass, trial number, the interaction between *ln* turning radius and *ln* pre-turn speed, *ln* turning radius and shelter orientation, *ln* pre-turn speed and surface friction, *ln* pre-turn speed and shelter orientation, and surface friction and trial number as fixed effects, and individual as a random effect. All continuous variables were *ln* transformed to satisfy the assumption of linearity. Only variables present in at least one of the averaged models (importance > 0) are reported in the table.

Table 3. Full output of model-averaged LMMs to predict the proportion of strides with a slip during the turn ($n = 151$).

Response: <i>arcsine square root</i> proportion of strides with a slip	Estimate	Standard Error	z value	P value	Importance
(intercept)	0.883	0.327	2.705	0.007*	
turning speed	3E-4	0.177	0.002	0.999	0.21
turning radius	-0.522	0.696	0.751	0.453	1.00
pre-turn speed	0.005	0.082	0.060	0.952	0.17
friction	0.507	0.295	1.719	0.086	1.00
shelter orientation	0.004	0.050	0.082	0.935	0.07
trial	-8E-4	0.006	0.135	0.892	0.02
turning speed · turning radius	0.042	0.152	0.278	0.781	0.10
turning speed · friction	0.015	0.168	0.090	0.928	0.04
turning radius · pre-turn speed	0.025	0.114	0.217	0.828	0.06
turning radius · friction	-0.072	0.595	0.121	0.904	0.35
turning radius · shelter orientation	-0.009	0.074	0.119	0.906	0.02
pre-turn speed · friction	0.005	0.056	0.096	0.924	0.02

The full model contained the *arcsine square root* proportion of strides with a slip as the response variable, turning angle, turning speed, turning radius, pre-turn speed, surface friction, shelter orientation, mass, trial number, and the interaction between turning angle and shelter orientation, turning speed and turning radius, turning speed and pre-turn speed, turning speed and surface friction, turning radius and pre-turn speed, turning radius and surface friction,

turning radius and shelter orientation, pre-turn speed and surface friction, pre-turn speed and shelter orientation, and surface friction and trial number as fixed effects, and individual as a random effect. Only variables present in at least one of the averaged models (importance > 0) are reported in the table.

Table 4. Full output of model-averaged LMMs predicting turning angle ($n = 151$).

Response: turning angle	Estimate	Standard Error	z value	P value	Importance
(Intercept)	27.214	32.962	0.826	0.409	
turning speed	6.759	22.596	0.299	0.765	1.00
turning radius	-19.244	32.740	0.588	0.557	1.00
pre-turn speed	13.917	16.427	0.847	0.367	1.00
friction	-2.858	20.331	0.141	0.888	1.00
shelter orientation	41.414	17.375	2.383	0.017*	1.00
mass	0.059	0.275	0.215	0.830	0.23
trial	-0.218	0.450	0.484	0.629	0.41
turning speed · pre-turn speed	-4.073	9.762	0.417	0.677	0.93
turning speed · turning radius	-8.391	11.195	0.750	0.454	0.96
turning speed · friction	-11.262	13.792	0.817	0.414	0.98
turning radius · pre-turn speed	8.647	16.487	0.524	0.600	0.98
turning radius · friction	17.334	12.962	1.337	0.181	1.00
turning radius · shelter orientation	-11.986	11.411	1.050	0.294	0.98
pre-turn speed · friction	5.680	10.745	0.528	0.598	0.95
pre-turn speed · shelter orientation	-10.543	9.007	1.171	0.242	0.98
friction · trial	0.069	0.408	0.168	0.867	0.15

The full model contained turning angle as the response variable, turning speed, turning radius, pre-turn speed, surface friction, shelter orientation, mass, trial number, the interactions between

turning speed and turning radius, turning speed and pre-turn speed, turning speed and surface friction, turning radius and pre-turn speed, turning radius and surface friction, turning radius and shelter orientation, pre-turn speed and surface friction, pre-turn speed and shelter orientation, and surface friction and trial number as fixed effects, and individual as a random effect. Only variables present in at least one of the averaged models (importance > 0) are reported in the table.

Table 5. Error for eight different friction limit models, expressed as a percentage of the observed data, for the high-friction ($n = 35$) and low-friction surface ($n = 5$).

Coefficient of friction	Error for high-friction surface (% of observed data)	Error for low-friction surface (% of observed data)
0.7	32.115	26.714
0.8	27.497	26.280
0.9	23.159	28.884
1.0	20.259	32.232
1.1	18.563	35.416
1.2	16.943	38.458
1.3	15.817	41.376
1.4	15.999	44.183

Error is the mean difference between the 99th percent percentile of the observed turning speeds and those predicted by each friction limit model, expressed as a percentage of the observed data. Only turns of radius ≤ 0.5 m where no slips were present were assessed. Friction limit models were of the form $v = \sqrt{(g \cdot r \cdot u)}$, where v is the maximum turning speed, g is the force due to gravity, r is the turning radius, and u is the coefficient of friction.

SUPPLEMENTARY INFORMATION

Table S1: Morphological dimensions of a subset of female buff-footed antechinus used in this study ($n = 12$).

Length	M \pm SE (mm)
Head	30.25 \pm 0.15
Body	64.09 \pm 1.02
Tail	83.80 \pm 1.17
Left forelimb	20.69 \pm 0.13
Left hind limb	25.06 \pm 0.12
Left forefoot	10.57 \pm 0.19
Left hind foot	16.21 \pm 0.14

Measurements were head length (nuchal crest to tip of snout), body length (nuchal crest to base of tail), tail length (base to tip of tail), left forelimb length (radius-ulna), left hind limb length (tibia-fibula), and left forefoot and hind foot lengths (heel to claw base).

Table S2. Ranking of \ln turning radius LMMs based on the likelihood of being the best model.

Response: \ln turning radius	<i>df</i>	<i>logLik</i>	<i>AIC_C</i>	ΔAIC_C	<i>w</i>
<i>Model</i>					
1. \ln pre-turn speed + friction + shelter orientation + (\ln pre-turn speed · friction) + (\ln pre-turn speed · shelter orientation)	8	-173.726	364.5	0	0.344
2. \ln pre-turn speed + friction + shelter orientation + \ln mass + (\ln pre-turn speed · friction) + (\ln pre-turn speed · shelter orientation)	9	-172.606	364.5	0.024	0.340
3. \ln pre-turn speed + friction + shelter orientation + (\ln pre-turn speed · shelter orientation)	7	-176.303	367.4	2.925	0.080
4. \ln pre-turn speed + friction + shelter orientation + \ln mass + (\ln pre-turn speed · shelter orientation)	8	-175.300	367.6	3.148	0.071
5. \ln pre-turn speed + friction + shelter orientation	6	-177.900	368.4	3.919	0.049
6. \ln pre-turn speed + friction + shelter orientation + \ln mass	7	-176.976	368.7	4.271	0.041
7. \ln pre-turn speed + friction + shelter orientation + (\ln pre-turn speed · friction)	7	-177.402	369.6	5.123	0.027
8. \ln pre-turn speed + friction + shelter orientation + \ln mass + (\ln pre-turn speed · friction)	8	-176.465	370.0	5.480	0.022
Full model (ranked 22nd) , \ln pre-turn speed + friction + shelter orientation + \ln mass + trial + (\ln pre-turn speed · friction) + (\ln pre-turn speed · shelter orientation) + (friction · trial)	11	-177.557	379.0	14.549	2E-4
Null model (ranked 59th) , intercept only	3	-211.192	428.6	64.081	4E-15

w is the Akaike weight, which equals the probability that the model describes the data better than the other models. Only models with an Akaike weight of at least 1% are listed, in addition to the full model and the null model. In addition to their fixed effects, all models contain individual as a random effect. Continuous variables were \ln transformed to satisfy the assumption of linearity.

Table S3. Ranking of *ln* turning speed LMMs based on the likelihood of being the best model.

Response: <i>ln</i> turning speed	<i>df</i>	<i>logLik</i>	<i>AIC_C</i>	ΔAIC_C	<i>w</i>
<i>Model</i>					
1. <i>ln</i> turning radius + <i>ln</i> pre-turn speed + friction	6	83.832	-155.1	0	0.713
2. <i>ln</i> turning radius + <i>ln</i> pre-turn speed + friction + <i>ln</i> mass	7	82.630	-150.5	4.605	0.071
3. <i>ln</i> turning radius + <i>ln</i> pre-turn speed + friction + (<i>ln</i> pre-turn speed · friction)	7	82.540	-150.3	4.784	0.065
4. <i>ln</i> turning radius + <i>ln</i> pre-turn speed + friction + (<i>ln</i> turning radius · <i>ln</i> pre-turn speed)	7	82.222	-149.7	5.421	0.047
5. <i>ln</i> turning radius + <i>ln</i> pre-turn speed	5	79.402	-148.4	6.692	0.025
6. <i>ln</i> turning radius + <i>ln</i> pre-turn speed + friction + shelter orientation	7	81.377	-148.0	7.110	0.020
7. <i>ln</i> turning radius + <i>ln</i> pre-turn speed + friction + shelter orientation + (<i>ln</i> turning radius · shelter orientation)	8	82.089	-147.2	7.918	0.014
Full model (ranked 160th) . <i>ln</i> turning radius + <i>ln</i> pre-turn speed + friction + shelter orientation + <i>ln</i> mass + trial + (<i>ln</i> turning radius · <i>ln</i> pre-turn speed) + (<i>ln</i> turning radius · shelter orientation) + (<i>ln</i> pre-turn speed · friction) + (<i>ln</i> pre-turn speed · shelter orientation) + (friction · trial)	14	68.571	-106.1	49.028	2E-11
Null model (ranked 252nd) . intercept only	3	-52.964	112.1	267.123	7E-59

w is the Akaike weight, which equals the probability that the model describes the data better than the other models. Only models with an Akaike weight of at least 1% are listed, in addition to the full model and the null model. In addition to their fixed effects, all models contain individual as a random effect. Continuous variables were *ln* transformed to satisfy the assumption of linearity.

Table S4. Ranking of presence of a slip GLMMs based on the likelihood of being the best model.

Response: presence of a slip	<i>df</i>	<i>logLik</i>	<i>AIC_C</i>	ΔAIC_C	<i>w</i>
<i>Model</i>					
1. turning speed + pre-turn speed + friction + shelter orientation + trial + (friction · trial)	8	-56.315	129.6	0.00	0.014
Full model (ranked 6367th). turning angle + turning speed + turning radius + pre-turn speed + friction + shelter orientation + trial + mass + (turning angle · shelter orientation) + (turning speed · turning radius) + (turning speed · pre-turn speed) + (turning speed · friction) + (turning radius · pre-turn speed) + (turning radius · friction) + (turning radius · shelter orientation) + (pre-turn speed · friction) + (pre-turn speed · shelter orientation) + (friction · trial)	20	-51.412	149.3	19.64	8E-7
Null model (ranked 7834th). intercept only	2	-103.488	211.1	81.41	3E-20

w is the Akaike weight, which equals the probability that the model describes the data better than the other models. Only models with an Akaike weight of at least 1% are listed, in addition to the full model and the null model. In addition to their fixed effects, all models contain individual as a random effect.

Table S5. Ranking of arcsine square root proportion of turning strides with a slip LMMs based on the likelihood of being the best model.

Response: arcsine square root proportion of turning strides with a slip	<i>df</i>	<i>logLik</i>	<i>AIC_C</i>	ΔAIC_C	<i>weight</i>
<i>Model</i>					
1. turning radius + friction	5	-35.793	82.6	0.00	0.251
2. turning radius + friction + (turning radius · friction)	6	-35.170	83.7	1.17	0.140
3. turning radius + pre-turn speed + friction	6	-36.316	86.0	3.46	0.044
4. turning speed + turning radius + friction	6	-36.336	86.1	3.50	0.044
5. turning speed + turning radius + friction + (turning speed · turning radius)	7	-35.201	86.3	3.730	0.039
6. turning radius + pre-turn speed + friction + (pre-turn speed · turning radius)	7	-35.443	86.8	4.214	0.031
7. turning speed + turning radius + friction + (turning radius · friction)	7	-35.680	87.3	4.689	0.024
8. turning radius + pre-turn speed + friction + (turning radius · friction)	7	-35.717	87.3	4.762	0.023
9. turning radius + friction + shelter orientation	6	-36.970	87.3	4.770	0.023
10. turning speed + turning radius + friction + (turning speed · turning radius) + (turning radius · friction)	8	-34.563	87.6	5.039	0.020
11. turning radius + friction + trial	6	-37.252	87.9	5.334	0.017
12. turning radius + pre-turn speed + friction + (pre-turn speed · turning radius) + (turning radius · friction)	8	-34.846	88.2	5.605	0.015
13. turning speed + turning radius + friction + (turning speed · friction) + (turning radius · friction)	8	-34.849	88.2	5.610	0.015
14. turning radius + friction + shelter orientation + (turning radius · shelter orientation)	7	-36.157	88.2	5.643	0.015
15. turning radius + pre-turn speed + friction + (pre-turn speed · friction)	7	-36.194	88.3	5.716	0.014
16. turning radius + friction + shelter orientation + (turning radius · friction)	7	-36.330	88.6	5.988	0.013
17. turning speed + turning radius + friction + (turning speed · turning radius) + (turning speed · friction) + (turning radius · friction)	9	-33.806	88.8	6.201	0.011

Full model (ranked 7889th) . turning angle + turning speed + turning radius + pre-turn speed + friction + shelter orientation + mass + trial + (turning angle · shelter orientation) + (turning speed · turning radius) + (turning speed · pre-turn speed) + (turning speed · friction) + (turning radius · pre-turn speed) + (turning radius · friction) + (turning radius · shelter orientation) + (pre-turn speed · friction) + (pre-turn speed · shelter orientation) + (friction · trial)	21	-46.494	155.5	72.951	4E-17
Null model (ranked 100th) . intercept only	3	-43.841	94.1	11.494	8E-4

w is the Akaike weight, which equals the probability that the model describes the data better than the other models. Only models with an Akaike weight of at least 1% are listed, in addition to the full model and the null model. In addition to their fixed effects, all models contain individual as a random effect. The proportional response variable was *arcsine square root* transformed to approximate a normal distribution.

Table S6. Ranking of turning angle LMMs based on the likelihood of being the best model.

Response: turning angle	<i>df</i>	<i>logLik</i>	<i>AIC_C</i>	ΔAIC_C	<i>w</i>
<i>Model</i>					
1. turning speed + turning radius + pre-turn speed + friction + shelter orientation + (turning speed · turning radius) + (turning speed · pre-turn speed) + (turning speed · friction) + (turning radius · pre-turn speed) + (turning radius · friction) + (turning radius · shelter orientation) + (pre-turn speed · friction) + (pre-turn speed · shelter orientation)	16	-590.222	1216.5	0	0.198
2. turning speed + turning radius + pre-turn speed + friction + shelter orientation + trial + (turning speed · turning radius) + (turning speed · pre-turn speed) + (turning speed · friction) + (turning radius · pre-turn speed) + (turning radius · friction) + (turning radius · shelter orientation) + (pre-turn speed · friction) + (pre-turn speed · shelter orientation)	17	-589.604	1217.8	1.307	0.103
3. turning speed + turning radius + pre-turn speed + friction + shelter orientation + mass + (turning speed · turning radius) + (turning speed · pre-turn speed) + (turning speed · friction) + (turning radius · pre-turn speed) + (turning radius · friction) + (turning radius · shelter orientation) + (pre-turn speed · friction) + (pre-turn speed · shelter orientation)	17	-589.873	1218.4	1.844	0.079
4. turning speed + turning radius + pre-turn speed + friction + shelter orientation + trial + (turning speed · turning radius) + (turning speed · pre-turn speed) + (turning speed · friction) + (turning radius · pre-turn speed) + (turning radius · friction) + (turning radius · shelter orientation) + (pre-turn speed · friction) + (pre-turn speed · shelter orientation) + (friction · trial)	18	-588.619	1218.4	1.917	0.076
5. turning speed + turning radius + pre-turn speed + friction + shelter orientation + mass + trial + (turning speed · turning radius) + (turning speed · pre-turn speed) + (turning speed · friction) + (turning radius · pre-turn speed) +	18	-589.267	1219.7	3.213	0.040

	(turning radius · friction) + (turning radius · shelter orientation) + (pre-turn speed · friction) + (pre-turn speed · shelter orientation)					
6.	Full model. turning speed + turning radius + pre-turn speed + friction + shelter orientation + mass + trial + (turning speed · turning radius) + (turning speed · pre-turn speed) + (turning speed · friction) + (turning radius · pre-turn speed) + (turning radius · friction) + (turning radius · shelter orientation) + (pre-turn speed · friction) + (pre-turn speed · shelter orientation) + (friction · trial)	19	-588.292	1220.4	3.883	0.028
7.	turning speed + turning radius + pre-turn speed + friction + shelter orientation + (turning speed · turning radius) + (turning speed · friction) + (turning radius · pre-turn speed) + (turning radius · friction) + (turning radius · shelter orientation) + (pre-turn speed · friction) + (pre-turn speed · shelter orientation)	15	-593.540	1220.6	4.133	0.025
8.	turning speed + turning radius + pre-turn speed + friction + shelter orientation + (turning speed · turning radius) + (turning speed · pre-turn speed) + (turning speed · friction) + (turning radius · pre-turn speed) + (turning radius · friction) + (turning radius · shelter orientation) + (pre-turn speed · shelter orientation)	15	-593.692	1221.0	4.446	0.021
9.	turning speed + turning radius + pre-turn speed + friction + shelter orientation + (turning speed · pre-turn speed) + (turning speed · friction) + (turning radius · pre-turn speed) + (turning radius · friction) + (turning radius · shelter orientation) + (pre-turn speed · friction) + (pre-turn speed · shelter orientation)	15	-593.891	1221.3	4.835	0.018
10.	turning speed + turning radius + pre-turn speed + friction + shelter orientation + (turning speed · turning radius) + (turning speed · pre-turn speed) + (turning speed · friction) + (turning radius · pre-turn speed) + (turning radius · friction) + (turning radius · shelter orientation) + (pre-turn speed · friction)	15	-594.041	1221.6	5.135	0.015
11.	turning speed + turning radius + pre-turn speed + friction + shelter orientation + (turning speed · turning radius) + (turning speed · pre-turn speed) +	15	-594.107	1221.8	5.266	0.014

(turning radius · friction) +
(turning radius · shelter orientation) +
(pre-turn speed · friction) +
(pre-turn speed · shelter orientation)

Null model (ranked 2841st). intercept only 3 -663.310 1332.8 116.280 1E-26

w is the Akaike weight, which equals the probability that the model describes the data better than the other models. Only models with an Akaike weight of at least 1% are listed, in addition to the full model and the null model. In addition to their fixed effects, all models contain individual as a random effect.